Innovations in optical microfluidic technologies for point-of-care diagnostics†

Frank B. Myers and Luke P. Lee*

Received 18th July 2008, Accepted 1st October 2008
First published as an Advance Article on the web 30th October 2008
DOI: 10.1039/b812343h

Despite a growing focus from the academic community, the field of microfluidics has yet to produce many commercial devices for point-of-care (POC) diagnostics. One of the main reasons for this is the difficulty in producing low-cost, sensitive, and portable optical detection systems. Although electrochemical methods work well for certain applications, optical detection is generally regarded as superior and is the method most widely employed in laboratory clinical chemistry. Conventional optical systems, however, are costly, require careful alignment, and do not translate well to POC devices. Furthermore, many optical detection paradigms such as absorbance and fluorescence suffer at smaller geometries because the optical path length through the sample is shortened. This review examines the innovative techniques which have recently been developed to address these issues. We highlight microfluidic diagnostic systems which demonstrate practical integration of sample preparation, analyte enrichment, and optical detection. We also examine several emerging detection paradigms involving nanoengineered materials which do not suffer from the same miniaturization disadvantages as conventional measurements.

Introduction

The potential role of microfluidics in point-of-care (POC) diagnostics is widely acknowledged, and many reviews have explored its potential applications in clinical diagnostics,[1] personalized medicine,[2] global health,[3,4] and forensics.[5] Despite this, relatively few successful commercial implementations have been demonstrated.[6] To realize the commercialization of microfluidic POC diagnostics, challenges in integrating low-cost, sensitive, and portable optical detection systems must be addressed. Furthermore, to demonstrate the practicality of new techniques, an effort should be made to integrate sample preparation from raw clinical samples and compare detection sensitivity to conventional methods. Here, we review optical microfluidic systems which address these goals and introduce novel techniques for realizing practical POC diagnostics.

Lateral-flow assays (LFAs) and electrochemical sensors dominate the POC diagnostics market today. Immunochromatographic LFAs, commonly called "dipstick tests," rely on capillary flow and qualitative visual readout. LFAs are commercially available for a variety of diagnostic tests (pregnancy, cardiac markers, infectious diseases, *etc.*). These devices are successful because they are inexpensive to manufacture, robust, and easy to use. Although sensitivity is relatively poor compared to conventional immunological laboratory assays (such as the enzyme-linked immunosorbent assay, ELISA), LFAs are ideal for applications where analyte abundance is relatively high, complex sample preparation is not needed, and

Biomolecular Nanotechnology Center, Berkeley Sensor and Actuator Center, Department of Bioengineering, University of California, Berkeley, CA, 94720. E-mail: lplee@berkeley.edu; Fax: +510-642-5835; Tel: +510-642-5855

† Part of a special issue on Point-of-care Microfluidic Diagnostics; Guest Editors—Professor Kricka and Professor Sia.

Frank B. Myers is a PhD student in the UCSF/UC Berkeley Bioengineering graduate program. His research involves the integration of optical and electronic devices into microfluidic platforms for medical diagnostics and quantitative cell biology. He obtained BS degrees in Electrical and Computer Engineering from North Carolina State University in 2006.

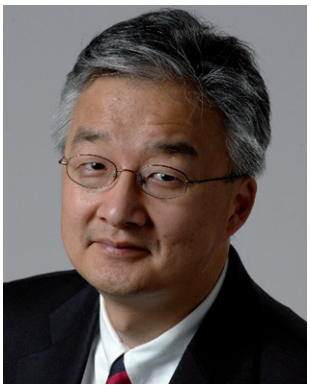

Luke P. Lee, PhD is the Lloyd Distinguished Professor of Bioengineering, director of the Biomolecular Nanotechnology Center, and co-director of the Berkeley Sensor and Actuator Center at UC Berkeley. He received his BA in Biophysics and PhD in Applied Physics from UC Berkeley. His current research interests include nanoplasmonics, lab-on-a-chip devices for quantitative biology and diagnostics, molecular biophysics, and integrative translational medicine.

a simple yes/no diagnostic is sufficient. In many cases, however, more sophisticated assays are required which call for multi-step protocols and complex fluid handling. Nucleic acid amplification and analysis is perhaps the most pertinent example, as more genotypic assays are emerging for pathogen detection and therapy prescription. For example, efforts are underway to develop genotypic POC assays for HIV,[7] tuberculosis,[8] and enteric diseases,[4] all of which are desperately needed in the developing world.

Electrochemical assays, on the other hand, have been very successful for quantitative analysis of certain small-molecule analytes, blood chemistry, and urinalysis. Conventional glucose meters are based on electrochemical detection methods, as is the handheld i-STAT used in hospital ICUs, which is capable of rapidly analyzing 25 different blood parameters (Fig. 1). However, electroactive enzyme labeling is generally required for proteins and nucleic acids, and background interference with non-specific redox species in the sample is a concern. Electrochemical techniques are heavily influenced by temperature variations at the electrode, chemical factors like pH and ionic concentrations, redox by-product accumulation near the electrodes, and electrode surface conditions—a factor which may limit the shelf life and require more stringent storage conditions for microfluidic disposables.

Because of the limitations of other techniques and the ubiquity of optical instrumentation in the laboratory, optical detection remains the preferred technique for quantitative proteomic or genomic diagnostics. Optical detection may have a per-test cost advantage over electrochemical detection because electrodes do not have to be integrated onto the disposable. Also, optical detection may be easier to multiplex since commercial CCD or CMOS image sensors could detect hundreds or thousands of simultaneous reactions at once, where each pixel corresponded to a different location on the detection array. Multiplexing on this scale is difficult to achieve with electrodes. While optical detection is quite straightforward in a laboratory environment where microscopes, lasers, spectrophotometers, lenses, and filters can be precisely arranged and aligned, these systems are difficult to miniaturize into a low-cost, portable, and robust system. Currently, most microfluidic devices are demonstrated using conventional optical systems. However, thanks to the rapid reduction in the cost of quality optoelectronic components like CCDs and laser diodes, as well as recent innovations in microfluidic integration and nanoscale materials for label-free biosensing, optical detection is becoming more practical for POC diagnostics.

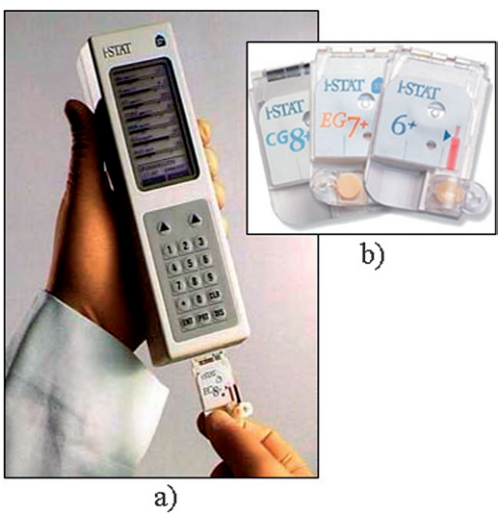

Fig. 1 (a) Abbott i-STAT electrochemical blood analyzer. (b) Disposable microfluidic assay cartridges. Reprinted with permission from Abbott Labs.

This review examines current research and product development in POC diagnostic devices which utilize optical detection within microfluidic platforms. We emphasize those efforts which demonstrate low-cost integration and quantitative results on real-world samples. The first half of the review focuses on the miniaturization of conventional optical measurements, both on-chip and off-chip, while the second half focuses on emerging detection paradigms which rely on nanoparticles and nano-engineered materials. We focus primarily on developments from 2005–2008.

Integrated optical systems

Conventional optical detection methods, including absorbance, fluorescence, chemiluminescence, interferometry, and surface plasmon resonance, have all been applied in microfluidic biosensors. However, optical detection generally requires expensive hardware which is difficult to miniaturize, and it suffers at lower length scales. The shorter optical path lengths through the sample reduce sensitivity and higher surface-to-volume ratios lead to increased noise from non-specific adsorption to chamber walls. To address these issues, many integrated optical systems are being explored in which waveguides, filters, and even optoelectronic elements are integrated onto the microfluidic device to improve sensitivity while reducing cost. In conjunction with these on-chip integrated components, many groups are incorporating low-cost optics, laser diodes, LEDs, CCD cameras, and photodiodes into portable diagnostic platforms. It's also worth noting that optical systems can not only be used for detection but also for actuation through various optical forces. Furthermore, through microscale manipulation of fluids one can achieve tunable and reconfigurable on-chip optical systems. These fascinating techniques have given rise to the new field of optofluidics, which has been reviewed elsewhere.[9,10] Here, we focus exclusively on detection methods.

Absorbance detection

UV/visible absorption spectroscopy is a well-established technique in macroscale analytical chemistry and laboratory diagnostics. In this technique, the attenuation of incident light as a function of wavelength is measured using a spectrophotometer. The resulting spectrum reveals peaks in absorption which can help identify the composition and concentration of the sample. In most cases, changes in optical density or color are sufficient for diagnosis, so instrumentation for absorbance measurements tends to be much simpler than for other methods. However, the major limitation with absorbance measurements in microfluidics is that as sample volumes decrease, the optical path length through the sample decreases, and this directly impacts sensitivity as described by the Beer–Lambert law.

One interesting way to address this problem is by incorporating "air mirrors" which take advantage of the refractive index difference between PDMS and air. In one example, air cavities were fabricated adjacent to the flow cell which reflected light back into the fluid (Fig. 2).[11] Biconvex microlenses for light collimation were also integrated, and the system showed an impressive limit of detection (LOD) of 41 nM for absorption measurements of fluorescein. Collimation lenses are necessary to achieve reasonable optical path lengths because light diverges from the source. Furthermore, stray light can reach the detector and reduce sensitivity. Ro *et al.* introduced planocovenx collimation lenses along with rectangular apertures to block stray light at both the input and output fiber channels.[12] They demonstrated a tenfold increase in sensitivity using this technique, but the device required a complicated three-layer PDMS fabrication process to realize the lenses, slits, and flow cell.

Steigert *et al.* developed a completely integrated centrifugal CD-based microfluidic system for alcohol detection from whole blood using absorbance measurements.[13] A cocktail of reagents were introduced which lead to the production of a colorimetric dye in the presence of ethanol. A laser was focused perpendicular to the cyclic olefin copolymer (COC) substrate where it was reflected 90 degrees into the detection chamber by a micropatterned V-groove adjacent to the chamber. Another V-groove on the opposite side reflected the light back to a spectrophotometer. This allowed the laser to interrogate the entire cross sectional length of the chamber (10 mm), enabling an LOD of 0.04% for ethanol, which is sufficient for the target applications in emergency medicine. The device leveraged a number of interesting microfluidic techniques unique to centrifugal systems, namely: capillary hold and burst valves for precise metering of sample and reagents, sample separation by centrifugation, and rapid mixing *via* oscillatory rotation. Furthermore, one could conceivably multiplex this assay by having multiple chambers around a single disk and synchronizing the laser/detector with the disk as it spins. This would allow a single fixed laser and photodiode to interrogate an entire array of chambers. Although CD-based microfluidics have their disadvantages, particularly when more complex valving is required, for many applications they are an attractive option, especially given the ease with which centrifugal separations can be integrated. Given their ubiquity and low cost, there is substantial interest in using conventional CD/DVD drives to perform molecular diagnostics. By functionalizing probe molecules onto the surface of CDs and observing the data error levels as a CD-ROM reads the disc, groups have shown that it is possible to colorimetrically detect ligand binding.[14,15] However, optical detection with a CD-ROM has yet to be shown with a microfluidic system integrated on the disc.

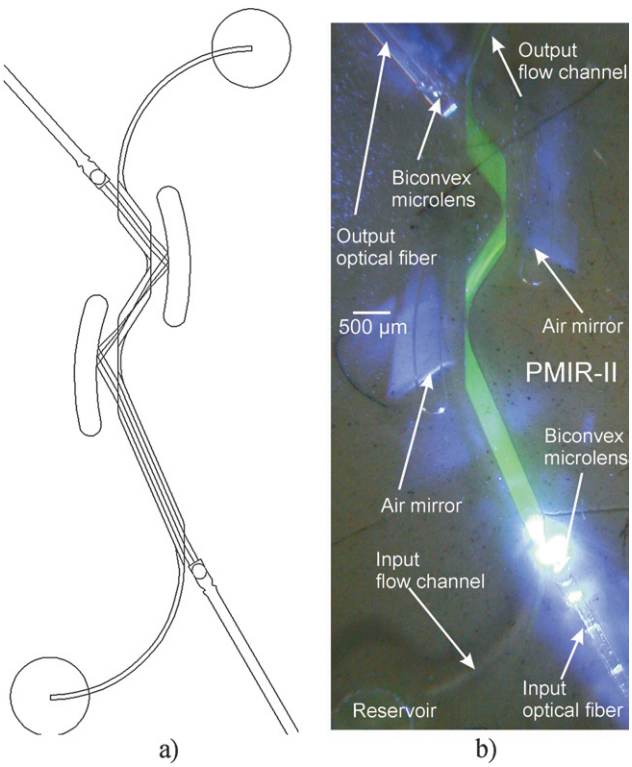

Fig. 2 Air mirrors and air lenses, which take advantage of the difference in refractive indices of PDMS and air, are positioned around an absorbance flow cell for increased optical path length. (a) Ray tracing diagram of two mirrors reflecting light through the flow cell. (b) Photograph showing fluorescein illumination in the channel. Reprinted from ref. 11 with permission from the Royal Society of Chemistry.

Since nucleic acids and proteins generally absorb strongly in the UV, absorption spectroscopy is commonly employed in liquid chromatography and electrophoresis to monitor the progression of biomolecules down a separation column in a label-free manner. Miniaturization provides a number of benefits for these techniques including higher separation efficiencies, reduced non-diffusional band broadening, reduced separation times, and reduced electric potentials (in the case of capillary electrophoresis). Gustoffson *et al.* integrated optical waveguides and a fluidic separation channel into a silicon substrate using a single etching step followed by thermal oxidation to form UV-transparent SiO_2 waveguides.[16] The separation channel consisted of micromachined pillars and was functionalized with octylsilane to facilitate electrochromatographic separation of electrically-neutral species. A glass lid containing fluidic access holes was fusion bonded on top of the oxidized silicon, forming closed channels. Two 90 degree bends in the channel allowed the waveguides to couple into a 1 mm straight segment at the distal end of the separation column. The waveguide structures featured micromachined fiber couplers at the end to ensure optimal alignment with external optical fibers. A major limitation of this fabrication procedure was that thermal oxidation led to rounding of the pillars which contributed to band broadening due to the non-uniform cross section along the height of the separation channel. Because of this, separation bands were an order of magnitude wider than previous microchip electrochromatography systems. Still, the device introduced an interesting design for integrated optics in microchip chromatography systems and a revision of the fabrication procedure could most likely improve device performance.

Despite the relatively poor sensitivity of absorbance measurements in microfluidics compared to fluorescence, its instrumentation simplicity gives it an advantage in certain applications. Indeed, several absorbance-based microfluidic POC products are available. The Nanogen i-Lynx, for example,

performs quantitative absorbance measurements on LFAs for monitoring cardiac markers.[17] Cholestech's GDX System uses a microfluidic disposable to measure glycosylated hemoglobin from whole blood.[18] The system performs lysis of red blood cells, affinity chromatography, and absorbance measurements to determine the ratio of glycosylated to non-glycosylated hemoglobin, an important diagnostic for diabetes patients.

Fluorescence detection

Fluorescence is the most common optical method for molecular sensing in microfluidic systems due to the well-established, highly sensitive, and highly selective fluorescent labeling techniques from conventional genomic and proteomic analysis. However, autofluorescence is a problem with many polymer materials as well as non-specific biomolecules in the sample, so material selection and sample purity are very important. Fluorescence is typically laser-induced, because lasers have a low divergence and can easily be focused into a small detection region. Furthermore, laser diodes are inexpensive and easily integrated into a portable device.[19–22] As an even lower cost alternative, LEDs can be used for fluorescence excitation. LEDs are less ideal because of their high divergence and relatively broad emission spectra, but many groups have shown good results with LED-induced fluorescence by incorporating integrated lenses, waveguides and filters into their microfluidic designs. Seo and Lee demonstrated a self-aligned 2D compound microlens which dramatically reduced spherical aberration compared to single-lens designs.[23,24] They showed that a 1 mm alignment offset of the LED corresponded to only an 8.4% decrease in fluorescence (Fig. 3). Furthermore, the fabrication was simple, requiring only a single layer of PDMS.

Liquid-core waveguide arrangements have been shown, where a capillary serves as both the fluid channel (often for capillary electrophoresis) and a waveguide for collecting fluorescence emission.[25] To further increase signal-to-noise ratio (SNR) in this configuration, Zhang *et al.* used a synchronized dual-wavelength LED modulation approach to subtract background noise from stray excitation light.[26] They demonstrated a 100-fold improvement in SNR over previous work, with an LOD of 10 nM for FITC-labeled arginine. LED and optical fibers have also been encapsulated directly into a PDMS device for capillary electrophoresis.[27] In this example, the epoxy housing of the LED was removed, and the LED was placed in close proximity to the flow cell with a short-pass filter in between. The authors demonstrated a 600 nM LOD for fluorescein.

Other groups have explored the possibility of implementing long-pass filters[28] and waveguides[29] directly in PDMS. In the case of filters, the PDMS pre-polymer is doped with an organic dye, and in the case of waveguides, a pre-polymer with a higher refractive index than the device material is chosen. Schmidt *et al.* demonstrated an innovative microfluidic fluorescence spectrometer for flow cytometry consisting of a linear variable optical band-pass filter sandwiched between a flow cell and a CMOS image sensor.[30] In this configuration, each pixel on the CMOS sensor corresponded to a different color, so as particles flowed down the channel, a complete spectrum could be observed (Fig. 4).

Other groups have attempted to completely integrate a fluorescent detection system on-chip. Vezenov *et al.* demonstrated a tunable optically pumped dye laser implemented in a microfluidic cavity.[31] Balslev *et al.* developed a monolithic optoelectronic/microfluidic hybrid platform incorporating an optically

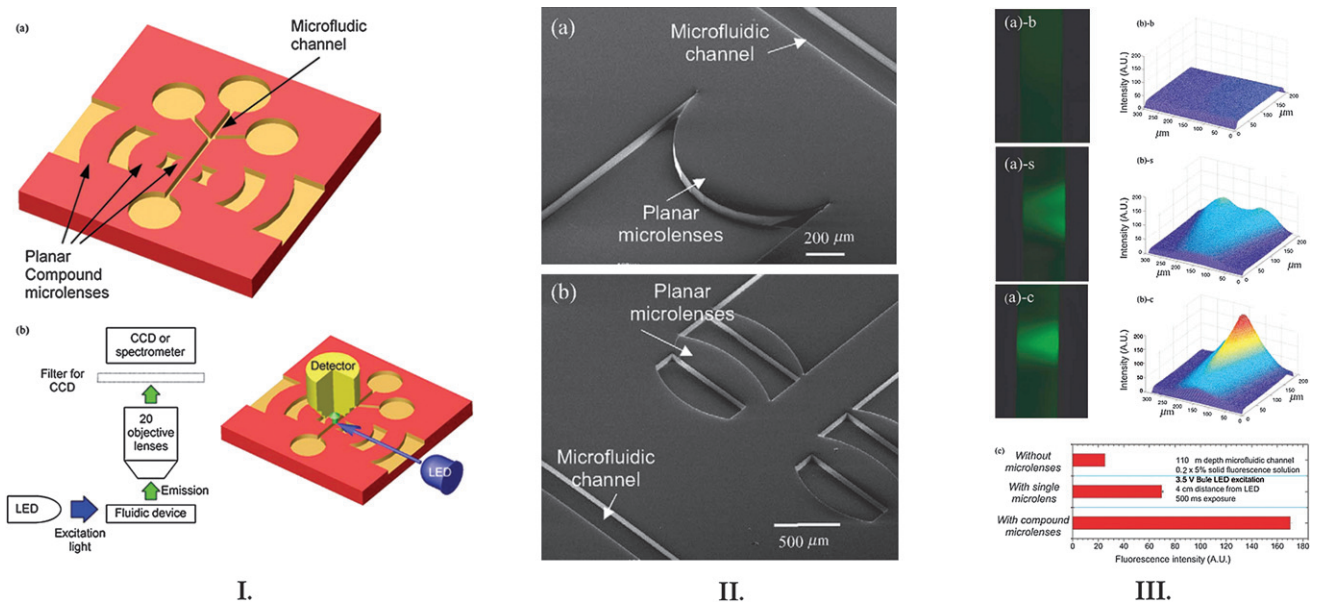

Fig. 3 Disposable integrated optical microfluidic device with self-aligned planar compound microlenses. (I) conceptual design of device showing (a) schematic of lenses and microfluidic channels and (b) experimental detection setup with LED. (II) SEM images of fabricated (a) single lens and (b) compound lens devices. (III) CCD images of fluorescent emission through single and compound microlenses. (a) Fluorescence images from microfluidic channel with LED excitation (b, s, and c denote 'without microlens', 'with single microlens' and 'with compound microlens', respectively). (b) Intensity profile of focused beam. (c) Relative fluorescent amplification showing best results are achieved with compound lens. Reprinted from ref. 24 with permission from Elsevier.

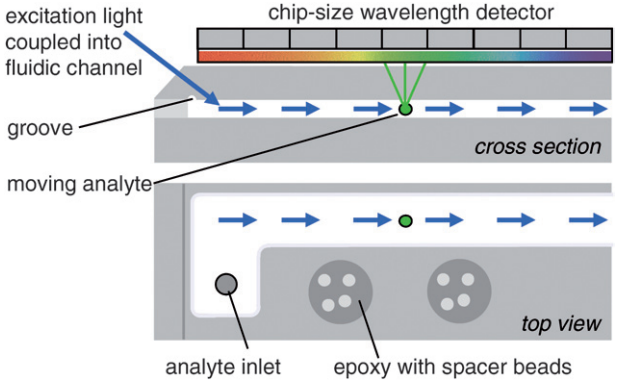

Fig. 4 Integrated on-chip fluorimeter. The wavelength detector (a linear CMOS image sensor) records the fluorescence spectrum of particles as they flow by. Reprinted from ref. 30 with permission from the Royal Society of Chemistry.

pumped dye laser, waveguides, fluid channels with passive mixers, and silicon photodiodes (Fig. 5).[32] Chediak *et al.* demonstrated a novel microassembly process for integrating (In, Ga)N blue LEDs, CdS thin-film filters, Si PIN photodetectors, and a PDMS microfluidic device (Fig. 6).[33] Monolithic integration of the entire optoelectronic system may not be the most cost-effective option when the device must be disposable. But as new manufacturing processes mature for organic optoelectronics which utilize low-cost solution deposition techniques, monolithic integration may become more attractive. Towards this vision, Pais *et al.* recently demonstrated a microfluidic device sandwiched between a planar organic LED and an organic photodiode. They characterized this device with rhodamine 6G (LOD of 100 nM) and fluorescein (LOD of 10 μM).[34] Although this detection limit is significantly higher than that achieved with conventional LEDs/photodiodes, organic optoelectronics are improving steadily and may soon represent a cost-effective alternative for detection in POC microfluidic devices.

In general, diagnostic sensitivity is directly related to the degree to which an analyte of interest can be concentrated within the detection region. In capillary electrophoresis (CE), for example, the more highly concentrated the "plug" of nucleic

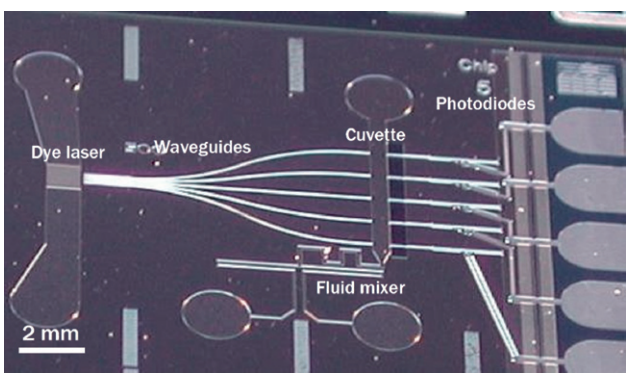

Fig. 5 An integrated optoelectronic/microfluidic detection system incorporating a dye laser, waveguides, microfluidic channels, and silicon photodiodes. Reprinted from ref. 32 with permission from the Royal Society of Chemistry.

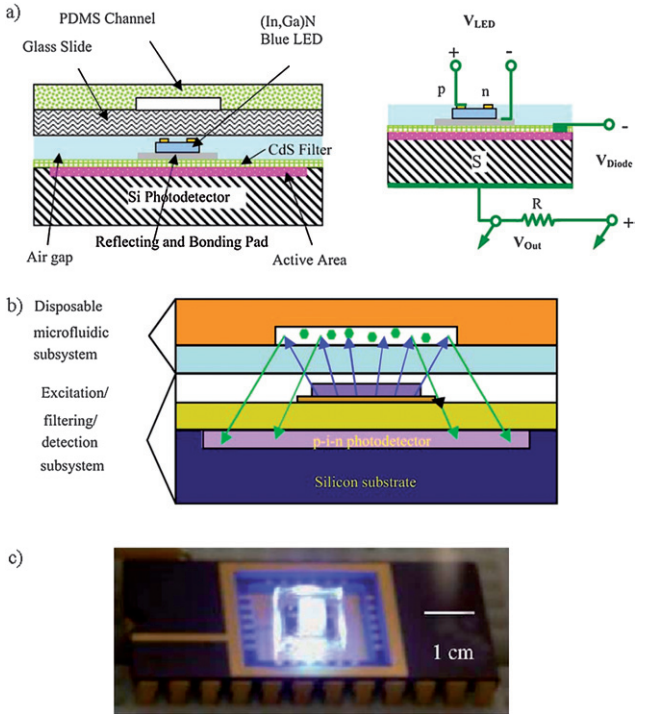

Fig. 6 (a) Schematic of the heterogeneous integration of a CdS filter with an (In, Ga)N LED, a Si PIN photodetector, and a microfluidic device. (b) Highlighting light paths for the excitation and Stokes-shifted emission signals. (c) Image of the prototype microsystem with the LED on and exciting the microfluidic device. Reprinted from ref. 33 with permission from Elsevier.

acids or proteins before electrophoretic separation, the more sharply defined the resulting separation bands will be. Herr *et al.* developed a preconcentration method for CE using *in-situ* photopolymerized gel membranes.[35] Fluorescently-labeled antibodies and analyte proteins were first electrophoretically driven against a region of gel with a relatively high degree of cross-linking (and therefore a smaller effective pore size) which acted as a size-exclusion membrane. The electric field was then switched, and the immunocomplexes and unbound antibodies flowed down a separation channel containing a gel with larger pores. This caused the antigen–antibody immunocomplexes and unbound antibodies to separate, and their relative fluorescent intensity was measured with a laser diode and PMT at a certain point on the channel. The ratio of bound to unbound antibodies correlated with protein concentration. This was incorporated into a portable saliva-based diagnostic platform for periodontal disease which included all optical elements.[22] In another example of how analyte preconcentration can greatly enhance sensitivity, Christodoulides *et al.* demonstrated a hundredfold LOD improvement over conventional ELISA diagnostics for the detection of C-reactive protein (CRP) in saliva.[36] Their device consisted of microwells etched in silicon which trapped agarose beads that were functionalized with CRP antibodies. A sandwich assay was performed on these beads. The microwells extended completely through the silicon substrate, and the sample and secondary labels were flowed perpendicular to the substrate (Fig. 7) *via* transparent PMMA manifolds. Because of this

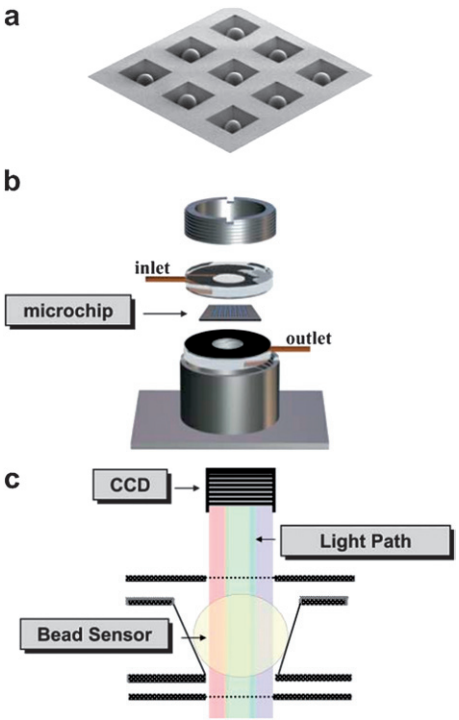

Fig. 7 (a) SEM image of a 3 × 3 array of agarose beads positioned in silicon microwells. (b) The microchip is sandwiched between two transparent PMMA inserts and packaged into a metal housing. (c) Schematic showing cross-sectional view of device with light path. Reprinted from ref. 36 with permission from the Royal Society of Chemistry.

configuration, CRP was forced into very close proximity with the beads, yielding excellent sensitivity.

Nucleic acid amplification and hybridization detection represent a growing field in microfluidic diagnostics. Conventionally, double-stranded DNA is most often detected using a fluorescent intercalating dye, so it is no surprise that this technique is also dominant in microfluidic systems. By far, the most common amplification technique employed is the polymerase chain reaction (PCR). Miniaturized PCR presents a number of advantages to conventional PCR: high thermal cycling rates (and therefore lower analysis times), low sample volumes, and integration with upstream sample preparation and downstream analysis components within a monolithic system to improve sensitivity and avoid sample contamination. On-chip PCR with capillary electrophoresis (CE) and fluorescent detection was first demonstrated by Woolley *et al.* in 1996,[37] and several recent examples have continued to improve on PCR with CE,[38,20,39] as well as hybridization detection.[40,41]

Liu *et al.* demonstrated a system for forensic analysis consisting of a glass microfluidic disposable for quadruplex Y-chromosome single tandem repeat (STR) typing which incorporated resistive heaters and pneumatic valves for performing on-chip PCR and CE detection.[20] A portable instrument was developed which contained power supplies for electrophoresis, a diode laser, an objective lens, and four dichroic filters and photomultiplier tubes (PMTs) for four-color fluorescent detection. They demonstrated the system with oral swab and human bone extracts, although sample preparation was performed off-chip. The system provided excellent detection sensitivity (down to 20 copies of DNA) with a 1.5 h run time. Another impressive system was demonstrated by Easley *et al.* which not only incorporated PCR and CE detection but also sample preparation and DNA/RNA purification. The device detected *Bacillus anthracis* from whole blood and *Bordetella pertussis* from nasal aspirate.[39] For fluorescent detection, the device employed external optics, a high-powered laser, and PMTs. Both of these systems are quite useful for certain applications (such as forensic labs), but in order to make them viable solutions for POC applications, more work is necessary to miniaturize, automate, and reduce the cost of the optical detection systems.

A complete handheld nucleic acid detection system has been developed which incorporates amplification not with PCR but with a lesser-known isothermal amplification technique called NASBA (nucleic acid sequence-based amplification). The system quantitatively detected the microorganism *Karenia brevis* using low-cost optical components including LEDs, photodiodes, and optical filters. Even temperature was maintained optically using an infrared heater and thermometer (Fig. 8).[42,43] The system was designed to interface with a PDA for real-time monitoring of fluorescence. Unfortunately, the LOD was not characterized, but nevertheless this is an impressive demonstration of practical, low-cost optical nucleic acid detection. NASBA, in fact, may be preferable to PCR for POC viral diagnostic applications because it does not require a reverse transcriptase step for RNA amplification.

In general, fluorescence remains the most widely used method of optical detection. Fluorescent detection has a number of advantages over other techniques, namely high sensitivity and a wealth of available fluorophores and labeling chemistries. However, fluorescent dyes remain rather costly, have a limited shelf life, and are often influenced by chemical factors such as pH which may vary from sample to sample. Furthermore, the

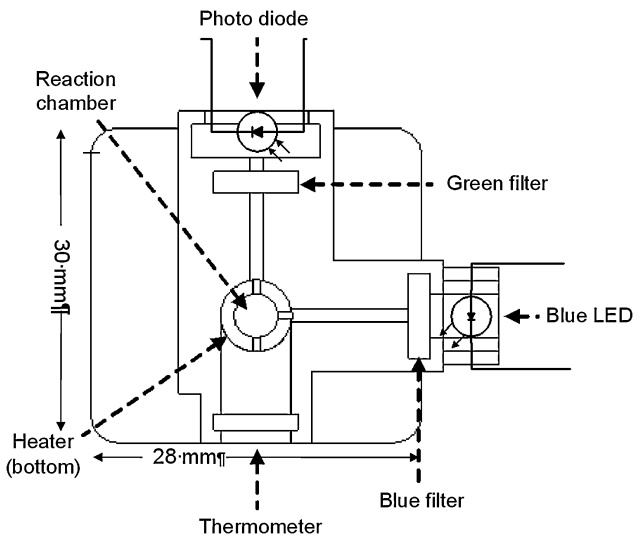

Fig. 8 Handheld NASBA detection system for *Karenia brevis*. The system uses an LED and photodiode for detection and an IR heater and thermometer to maintain temperature. Reprinted from ref. 43 with permission from SPIE.

labeling step itself requires complex fluid handling, mixing, and washing, which is difficult to automate in a rapid assay. For this reason, label-free analysis techniques which approach the sensitivity and specificity of fluorescent labeling are highly sought-after.

Chemiluminescence detection

Chemiluminescence is another attractive option for detection in which analyte binding causes photochemical emission, either directly or with the help of an enzyme label. The advantage of this technique for POC applications is that excitation instrumentation is not required, and therefore background interference is virtually eliminated. However, very sensitive detectors are typically required. Bhattacharyya and Klapperich developed a disposable microfluidic chemiluminescent immunoassay for detecting CRP in serum.[44] Their device demonstrated excellent correlation with conventional ELISA measurements throughout the clinically relevant range, with an LOD of 0.1 mg/L when using an external photomultiplier tube (PMT) luminescent reader. Their assay time was 25 min (compared to >12 h for ELISA). They also demonstrated proof-of-concept detection with an integrated photo-sensitive film, although they did not evaluate the LOD of this method. Yacoub-George *et al.* developed a multiplexed chemiluminescent capillary enzyme immunoassay sensor capable of simultaneously detecting toxins, bacteria, and viruses.[45] The assay was completed in 29 min. Using PMTs, they demonstrated LODs of 0.1 ng/mL for *staphylococcal enterotoxin B*, 10^4 colony-forming units per mL for *E. Coli* O157:H7, and 5×10^5 plaque-forming units per mL for bacteriophage M13.

Marchand *et al.* demonstrated a disposable microfluidic card with an integrated commercial CMOS active pixel sensor (APS) functionalized with DNA oligonucleotide probes for chemiluminescent hybridization detection.[46] Since the probes are directly attached to the sensor surface, this offers excellent photonic capture efficiency. The form factor of the device was equivalent to "smart card" credit cards, leveraging existing pick-and-place manufacturing technology for the integration of the CMOS chip (Fig. 9). However, although the cost of silicon CMOS image sensors continues to fall, it is difficult to say if they will become inexpensive enough to be incorporated on a disposable for POC applications. But if such a platform could be regenerated and reused, this might be a very attractive option for genomic analysis.

Interferometric detection

Interferometric sensing potentially offers label-free detection with very high sensitivity. In general, interferometric biosensor techniques rely on the splitting of a single coherent light source into two paths. Both paths are adjacent to the sample media, but only one is functionalized to be sensitive to the analyte of interest. Analyte binding causes a refractive index change along this optical path, resulting in a phase shift with respect to the non-functionalized reference path. This phase shift can have

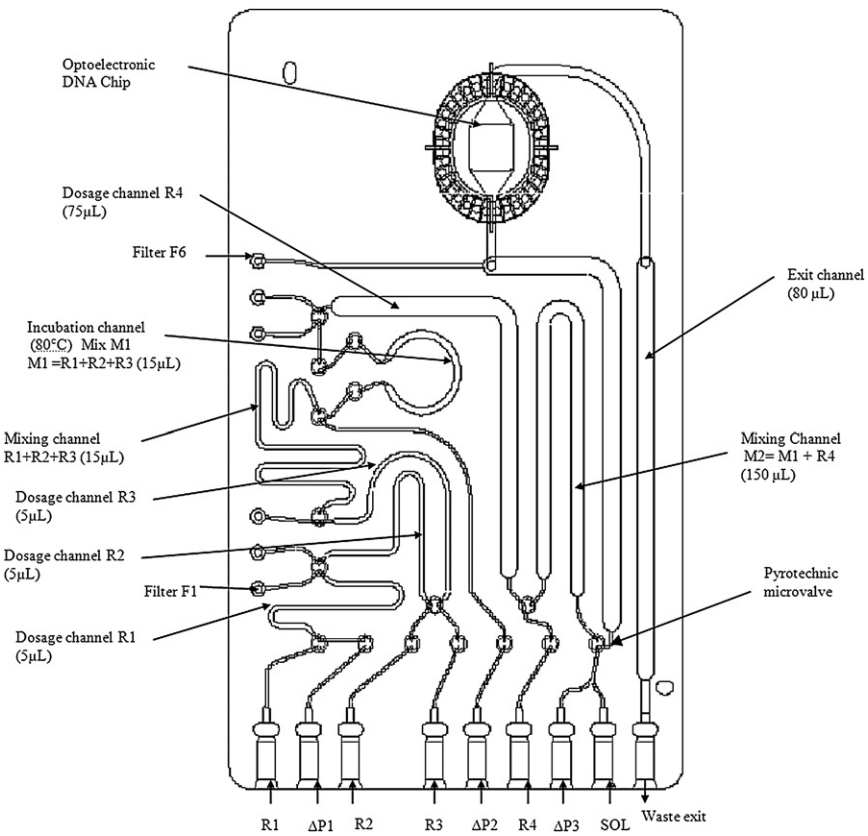

Fig. 9 An integrated optoelectronic/microfluidic DNA microarray incorporating a CMOS active pixel sensor in a smart card form factor. Reprinted from ref. 46 with permission from Springer.

a dramatic effect on the interference pattern resulting from the projection of these two beams, so by imaging this interference pattern, one can directly observe binding events. The reference path is what gives interferometry its sensitivity because it accounts for common-mode interference such as non-specific adsorption, temperature fluctuations, and intensity fluctuations. Ymeti *et al.* demonstrated an immunosensor using a Young interferometer configuration in which a microfluidic chip with integrated waveguides projected an interference pattern onto a CCD image sensor (Fig. 10).[47] In this device, three waveguides were functionalized with different antibodies and one waveguide was non-functionalized and served as a reference. When antigens bound, they interacted with the evanescent wave at the surface of the waveguide, changing the refractive index and leading to a shift in the interference pattern. The sensor was evaluated with herpes simplex virus. The sensor demonstrated a response time of just a few minutes and an LOD in the femtomolar range, approaching a single virion. Another report describes a similar Young interferometer biosensor assay to detect avian influenza (H5N1).[48] One potential drawback of interferometers of this type is that the micromachined geometries and material properties of the waveguides must be precisely matched.

Blanco *et al.* developed a biosensor based on a Mach–Zehnder interferometer which was implemented in a CMOS-compatible silicon process and was integrated with SU-8 microfluidic channels.[49] The advantage of the Mach–Zehnder configuration is that the interfering light paths are recombined on the device so that only an intensity variation is measured at the output. However, because this configuration requires monomode propagation, a 4 nm silicon nitride core was used in the waveguide which led to substantial insertion loss (9 dB) when coupled with external fibers.

Reflectometric interferometry is another method which can very precisely detect analyte binding at a surface. In this method, a laser is projected towards a functionalized surface and the reflected interference pattern is measured. Pröll *et al.* used this method to measure oligonucleotide hybridization. Because interferometry is less sensitive to temperature variations that other methods, they were able to perform melting curve studies and identify single nucleotide polymorphisms (SNPs) with single base-pair resolution.[50] The same group recently demonstrated this method for immunological detection.[51]

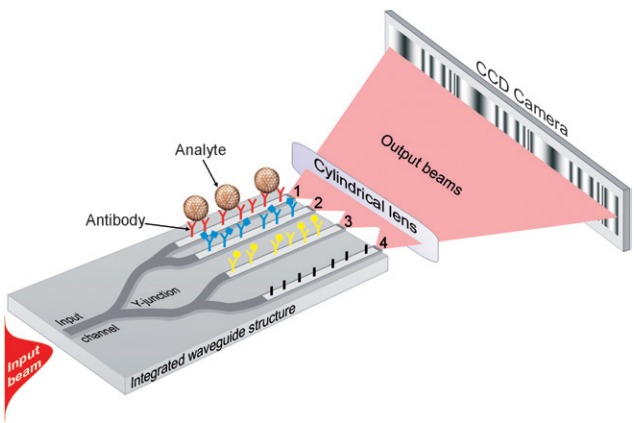

Fig. 10 A biosensor based on a Young interferometer in which analyte binding causes a change in the interference pattern projected onto a CCD camera. Reprinted from ref. 47 with permission from the American Chemical Society.

Back-scattering interferometry was demonstrated in a rectangular PDMS microfluidic channel, in which the walls of the channel caused light to interfere and produce fringe patterns whose position depended on the refractive index at the channel floor. An inexpensive, low-power, unfocused light source was used. By functionalizing the channel floor, the authors achieved femtomolar detection limits for both streptavidin–biotin and protein A-IgG immunodetection.[52] More recently, the same group demonstrated that the technique could also be applied to detect molecular binding in free solution rather than at a functionalized surface (Fig. 11).[53] Because surface functionalization is laborious, expensive, and limits device shelf life, free solution techniques are appealing. The authors were able to detect interaction of calmodulin with the protein calcineurin as well as Ca^{2+} ions, a small molecule inhibitor, and the M13 peptide. Furthermore, they detected immunocomplex formation between interleukin-2 and its antibody as well as protein A with IgG. The technique showed remarkable sensitivity; for interleukin-2, the authors estimate a detection limit of just 12 600 molecules. The major drawback of this technique is that because it is a volumetric measurement it may not be suitable for complex samples (such as human serum) which have other constituents that might affect bulk refractive index.

Surface plasmon resonance detection

Surface plasmon resonance (SPR) detection relies on the measurement of a refractive index change at a metal surface which has been functionalized with probe molecules. When light is incident on a thin metal film at a specific angle through a prism (Kretschmann configuration), it excites a propagating surface plasmon at the surface of the metal. At this angle, the reflectance intensity decreases sharply. This SPR angle is highly sensitive to the dielectric environment on the opposite side of the metal, so when ligands bind to the surface of the metal, they cause this SPR angle to change. The angle is measured either by rotating a narrowly-focused laser beam and looking for a reflectance minimum or by using a slightly divergent laser beam and imaging the reflectance angle spectrum exiting the prism.

Several laboratory-scale SPR detection systems for immunosensing and DNA hybridization detection exist, most notably the Biacore from GE Healthcare. Recently, efforts have focused on reducing the size and complexity of SPR sensors using integrated microfluidic systems. The Sensata Spreeta SPR sensor is a commercially available, low-cost SPR sensor which can be adapted to a variety of applications (Fig. 12).[54] The device provides an impressive LOD of 80 pM when tested with IgG. Waswa *et al.* demonstrated the use of the Spreeta for the immunological detection of *E. coli* O157:H7 in milk, apple juice, and ground beef extract.[55] They showed an LOD of 10^2 colony-forming units per mL and demonstrated that the sensor was non-responsive to other organisms (*E. coli K12 and Shigella*). *E. coli* is an enteric pathogen which poses a serious health risk and must be monitored closely in the food supply. Conventional methods rely on culturing which takes 1–3 days, a high degree of expertise, and specialized facilities. The Spreeta sensor was able to reliably quantify *E. coli* in 30 min. A similar assay was carried out by

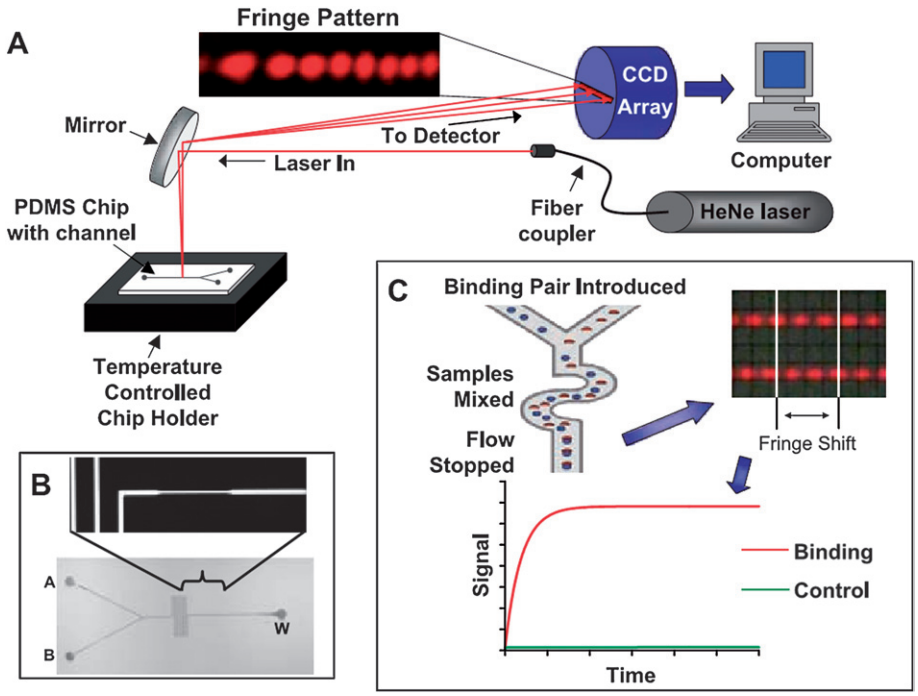

Fig. 11 Back-scattering interferometry through a rectangular PDMS channel produces fringe patters which correspond to antigen–antibody binding within the channel volume. No surface functionalization is necessary. (A) Optical elements of the system. (B) Photograph of microfluidic device with closeup of constriction region used for mixing. (C) Diagram showing device operation and observed fringe shift resulting from binding. Reprinted from ref. 53 with permission from the American Association for the Advancement of Science.

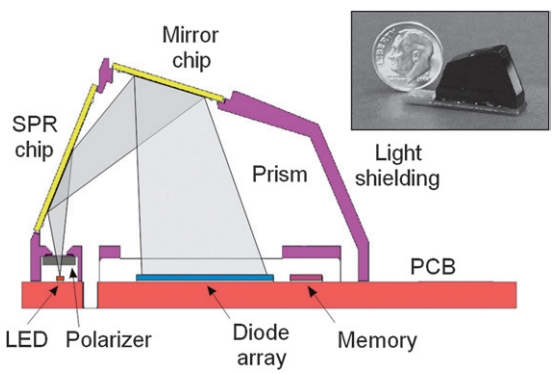

Fig. 12 Cross-sectional view of the Sensata Spreeta SPR sensor. Inset shows photograph of actual device. Reprinted from ref. 54 with permission from Elsevier.

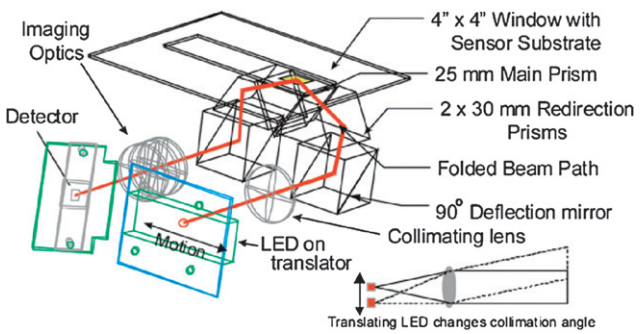

Fig. 13 Schematic of an integrated optical system for a breifcase-sized portable immunosensor based on SPR. Reprinted from ref. 57 with permission from Elsevier.

Wei *et al.* using the Spreeta to detect *Campylobacter jejuni* in poultry meat.[56]

Chinowsky *et al.* developed a portable briefcase-style SPR immunosensor platform (Fig. 13).[57] The system uses a folded light path incorporating a range of optical elements (mirrors, prisms, lenses) and an LED light source which is translated mechanically in order to generate the reflection spectrum on a CCD. A unique microfluidic card made of a combination of laser-cut laminated Mylar sheets, PDMS, and glass incorporates a diffusion-based H-filter, a herringbone micromixer, and gold-coated SPR detection regions. The materials were carefully chosen with manufacturability and cost in mind.[4] The sensor was demonstrated for phenytoin detection from saliva.[58] The sensitivity of the system is comparable to that obtained with the commercial Biacore system. Another briefcase-style sensor was developed by the same group which was capable of simultaneously detecting small molecules, proteins, viruses, bacteria, and spores.[59]

Recently, Feltis *et al.* demonstrated a low-cost handheld SPR-based immunosensor for the toxin Ricin (Fig. 14).[60] They demonstrated an LOD of 200 ng/mL. Although this is substantially higher than the LOD obtained with the Biacore sensor (10 ng/mL), it is quite sufficient for this particular application (200 ng/mL is 2500 times lower than the minimum lethal dose), and the result is available in 10 minutes.

Luo *et al.* developed a multilayer PDMS array consisting of multiple gold spots for the real-time observation of immunocomplex formation using SPR.[61] By using gold nanoparticles as

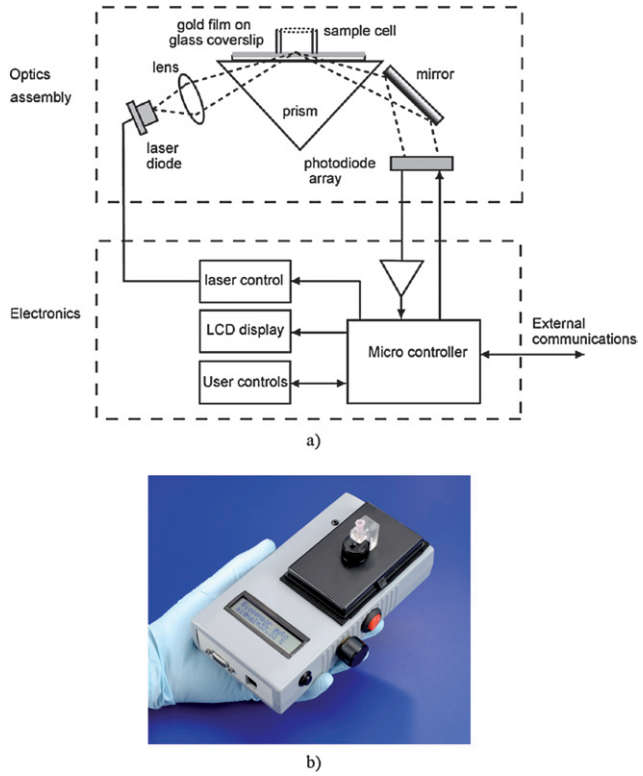

Fig. 14 Integrated SPR sensor for Ricin detection. (a) System diagram showing optical and electronic components. The system incorporates a laser diode, right angle prism, and photodiode array for detection. (b) Photograph of prototype handheld device. Reprinted from ref. 60 with permission from Elsevier.

secondary labels in a sandwich assay format, they demonstrated an LOD of ~38 pM with biotin-BSA/anti-biotin as the antigen/antibody pair. There was a tradeoff, however, between assay time and sensitivity. Without the nanoparticles, the LOD was 0.21 nM, but the assay took only 10 min to complete, compared to 60 min for the case with nanoparticles.

SPR is a well-established technique with excellent sensitivity. However, the instrumentation required is a bit complex, and a layer of metal (typically gold) must be deposited on the disposable device, thus raising cost. Also, the technique suffers from a strong temperature dependence.

Nanoengineered optical probes

Nanoengineered materials are emerging as powerful aids to optical detection. New labels such as quantum dots and up-converting phosphors have been developed which offer tunabilities, intensities, and longevities better than conventional organic dyes. Other approaches leverage the localized surface plasmon resonance (LSPR) effect to create highly sensitive sensors that depend not on sample volume but on near-field surface interactions, which make them excellent candidates for miniaturized systems.

Quantum dots

Quantum dots (QDs) are fluorescent semiconductor particles with finely tunable narrow-line emission spectra. This makes them ideal for multiplexed detection, potentially eliminating the need to immobilize capture probes in a spatial array. Not only would this reduce fabrication cost, but since diffusion times severely limit the throughput of conventional microarrays, this would provide a significant advantage for rapid diagnostics. Also, compared to organic dyes, quantum dots are brighter, do not photobleach, and are more resistant to chemical degradation.[62] Quantum dot "barcoding" is a popular technique employed in recent years in which combinations of quantum dots with different emission peaks are encapsulated in polymer microbeads such that as many as 10^6 unique biosensor probes, each functionalized with a different capture antibody or oligonucleotide, can be realized. Importantly, all of these barcodes can be excited with one wavelength. So, when used with a secondary fluorescent label, analyte binding of multiple barcodes can be measured simultaneously, without *a priori* knowledge of spatial arrangement. This technique was recently applied in a multiplexed microfluidic biosensor for the simultaneous detection of HIV, HBV, and HCV (Fig. 15).[63] A similar technique was applied for gene expression analysis in which 100 different genes were detected simultaneously with QD barcodes with detection limit, dynamic range, and analysis time all an order of magnitude better than conventional microarray methods.[64] Quantum dots do have their problems, however. They are relatively difficult to synthesize and functionalize and are consequently much more expensive than fluorophores. Also, they suffer from a limited shelf life. There are only a few examples of quantum dots being used as biosensors in microfluidics,[63,65–67] and no examples integrating them into portable POC diagnostic devices.

Up-converting phosphors

A new labeling technique currently being commercialized by OraSure Technologies is up-converting phosphor technology (UPT).[68–71] This technique involves using ceramic nanospheres containing rare earth metals which absorb multiple photons of infrared light for each emitted photon in the visible spectrum (anti-Stokes shift). Since this phenomenon bears no natural analog in most materials or biological media, it provides excellent SNR as compared with fluorescence, which is often limited by autofluorescence. Furthermore, UPT particles are available in different colors, are excited in the near IR range (where absorption from biological media is minimal), and do not fade or photobleach. UPT has been demonstrated for bacterial and viral identification using both genetic[69,71] and immunological[68,70] methods (Fig. 16). These examples use nitrocellulose LFA strips and a portable reader which detects the UPT particles with an IR laser diode and a PMT.

Silver-enhanced nanoparticle labeling

A novel method for DNA microarray analysis was introduced in 2000,[72] whereby gold nanoparticles are used as secondary labels and then subsequently enlarged *via* catalytic silver deposition to the point that they can be imaged using a conventional camera or slide scanner. It was further shown that the same technique could be applied to protein detection.[73] This technique has huge implications for POC diagnostics. For DNA analysis, it is so sensitive that it does not require nucleic acid amplification,

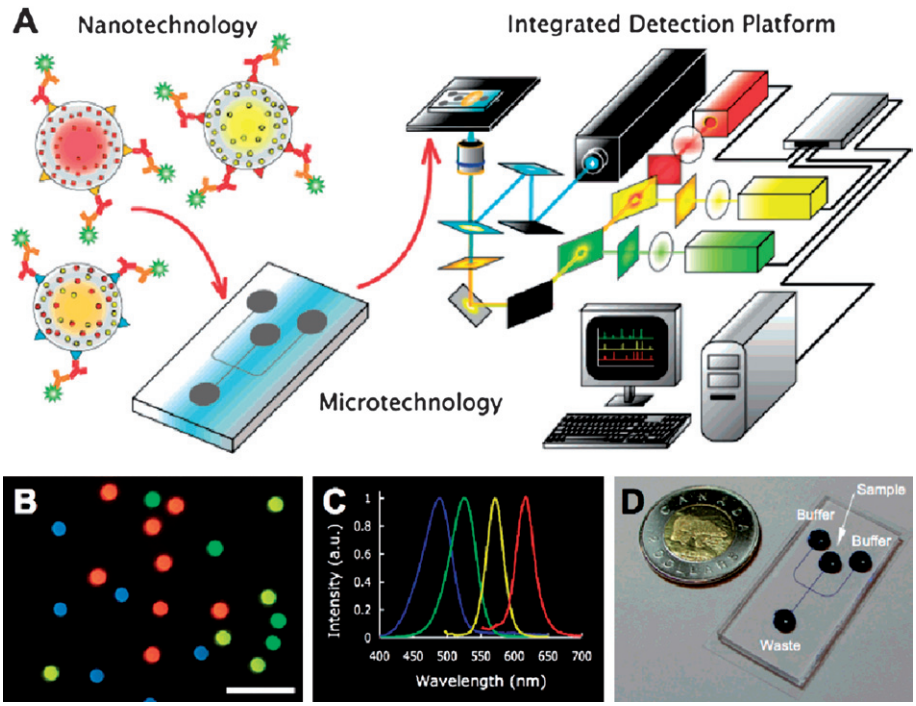

Fig. 15 (A) Quantum dot barcodes are used for multiplexed immunosensing in a microfluidic device with external optical detection. (B) Fluorescent image of quantum dots on chip. (C) Quantum dot emission spectra. (D) Fabricated microfluidic chip. Reprinted from ref. 63 with permission from the American Chemical Society.

greatly simplifying the instrumentation required. It also allows for simultaneous detection of DNA and proteins in the same array using the same processing steps. Recently, the technique has been commercialized by Nanosphere. The company received FDA approval in 2007 for its Verigene platform to be used in two genetic tests, one to identify markers for blood coagulation disorders and the other to assess a patient's candidacy for associated medication. Whole blood is dropped in a disposable cartridge which contains all required reagents for sample preparation, nanoparticle labeling, and silver deposition. The processing is completely automated and results are read using a slide scanner. The complete test takes only 90 minutes.

Localized surface plasmon resonance

Biosensors based on the localized surface plasmon resonance (LSPR) phenomenon represent one of the most active research areas in optical microfluidic biosensors today, and several reviews on this topic have been presented recently.[74–76] LSPR refers to the collective resonant oscillation of conduction electrons at the surface of a metal nanoparticle under the perturbation of incident light. Whereas conventional SPR sensing requires a prism or grating coupler to excite propagating plasmons on the surface of a metal, LSPR sensing requires no special coupling instrumentation and is typically performed with a white light source. A recent review compares biosensing

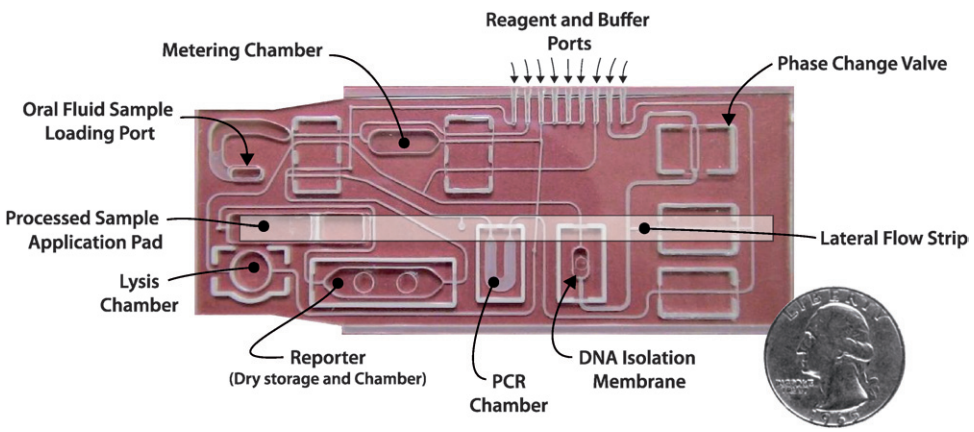

Fig. 16 Integrated saliva-based diagnostic platform incorporating sample prep, PCR, and UPT in a lateral flow detection strip. Reprinted from ref. 71 with permission from Blackwell Publishing.

with localized *versus* propagating surface plasmons.[77] The specific resonant frequency of a particle depends on the nanoparticle's size, shape, composition, and, most importantly for biosensing, the molecules in close proximity with the particle. This resonance leads to highly enhanced scattering at a specific wavelength. When molecules bind to the surface of the nanoparticle, they cause marked shifts in this resonance. LSPR is therefore label-free: it directly transduces a binding event to a spectral shift. Because LSPR sensing is a near-field phenomenon (<20 nm), it is less sensitive to background interference (*e.g.* from non-specific adsorbates on chamber walls) than absorbance or fluorescence. LSPR scattering is also very intense. For example, as pointed out by Anker *et al.*, the LSPR scattering cross-section of a gold nanoparticle is a millionfold greater than that of a single fluorescein molecule, and a thousandfold greater than an equivalent volume of fluorescein.[75] LSPR measurements are generally based on spectroscopic or refractive index changes rather than intensity changes, and are therefore less sensitive to background noise and normalization error from instrumental, chemical, or environmental variations as compared with conventional optical detection.[78] LSPR biosensing can be performed on ensembles of nanoparticles as well as individual particles. Many structures for LSPR have been explored, but few practical POC implementations have been shown. This is mainly due to the difficulty in producing nanoscale structures and particles which are sufficiently uniform and robust. Research has focused on developing new low-cost bulk fabrication methods for LSPR substrates and developing new surface treatment chemistries, particularly thiol-anchored self-assembled monolayers (SAMs), to improve nanoparticle stability.[75]

Pioneered by Van Duyne's group, nanosphere lithography (NSL) has emerged as one of the most promising techniques for bulk, high-uniformity manufacturing of LSPR structures on a flat substrate, particularly for surface-enhanced Raman scattering.[79] In this technique, silica or polystyrene nanospheres self-assemble into close-packed monolayers on a substrate and act as a shadow mask for metal deposition. Since the initial

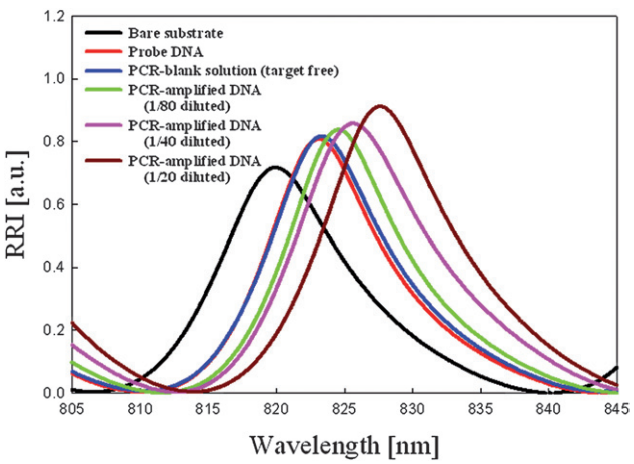

Fig. 17 LSPR wavelength shift due to DNA hybridization on the surface of a gold nanoparticle, showing various dilutions of PCR product. Reprinted from ref. 90 with permission from the American Chemical Society.

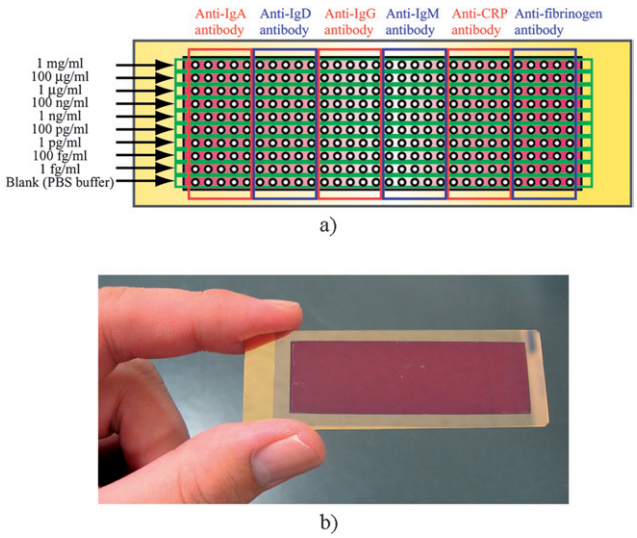

Fig. 18 (a) An LSPR-based biosensor array with 300 different spots for different concentrations of antibodies for IgA, IgD, IgG, IgM, CPR, and fibrinogen. (b) Photograph of fabricated device. Reprinted from ref. 82 with permission from the American Chemical Society.

demonstration of NSL, several innovative structures have been demonstrated using this technique including nanocrescents,[80] nanodisks,[81] films-over-nanospheres (FONs),[82,83] and triangular

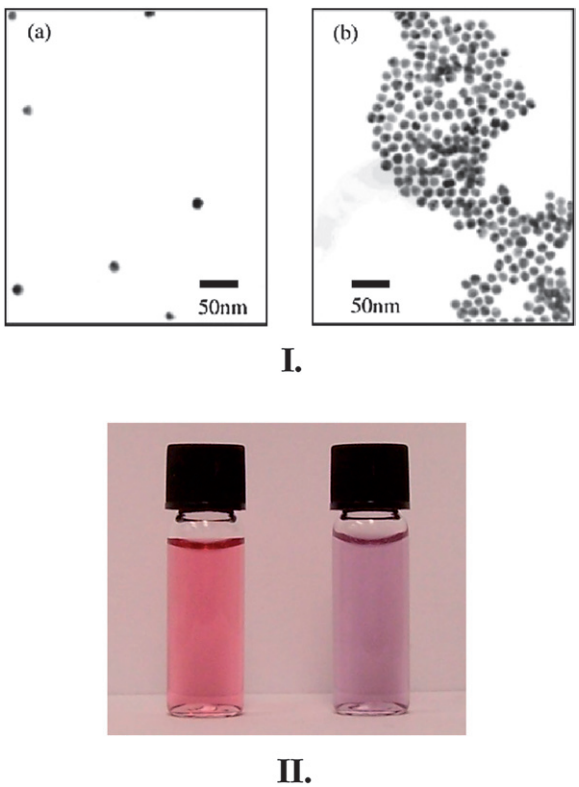

Fig. 19 LSPR detection based on ligand-induced gold nanoparticle aggregation. The resulting color change can be seen with the naked eye. (I) shows TEM images of aggregation while (II) shows resulting color change of sample solution. (a) Without cholera toxin. (b) With cholera toxin. Reprinted from ref. 86 with permission from the American Chemical Society.

prism arrays.[79,84] Despite the performance and simplicity of the NSL technique, it still does not achieve wafer-level uniformity because self-assembly of nanoscale colloids only provides defect-free areas of 10–100 μm^2. Wafer-scale fabrication of plasmonic substrates is currently a major area of research. Other groups have explored chemically synthesized colloidal particles including nanospheres,[85,86] nanorods,[78,87] nanoshells,[88] and nanorice.[89] These are attractive for POC diagnostics because they can be introduced into the device after its been manufactured, allowing a single device to be mass produced for a variety of different applications.

LSPR biosensors have been demonstrated for detecting DNA hybridization (Fig. 17),[82,90] antigen/antibody binding,[78,83,82] and small molecules.[85,86] In one excellent example of LSPR integration in a biosensor, Endo *et al.* created a multiplexed microarray biochip based on the FON technique for measuring immunoglobulins, CRP, and fibrinogen.[82] They used a nanospotter to deposit 300 different antibody spots on the array (Fig. 18), and achieved a detection limit of 100 pg/mL. The same group previously demonstrated a sensor for detecting casein from whole milk.[83] Gold nanorods immobilized on a substrate were also used for the detection of a model protein (streptavidin) in blood serum.[87] Schofield *et al.* showed that ligand-induced colloidal aggregation of GNPs upon binding of cholera toxin provided a dramatic shift in LSPR wavelength, such that the resulting color change could easily be distinguished with the naked eye (Fig. 19).[86] Recently, Hiep *et al.* demonstrated an LSPR biosensor on a microfluidic device,[91] but portable, fully-integrated diagnostic systems incorporating sample preparation and spectroscopic detection have yet to be realized. Probably the main reason for this is that very sensitive spectrophotometers are required to resolve the relatively small spectral shifts. For example, Fig. 14 shows that for that particular device there is only a ~5 nm shift in LSPR wavelength between the hybridized and unhybridized cases. This kind of distinction would be difficult to resolve with a low-cost, portable spectrophotometer.

SPR with nanohole gratings

As with LSPR sensors, SPR sensors based on propagating plasmons can also benefit from nanofabrication and nanoscale optics. Nanohole gratings have been studied as possible substitutes to smooth metal surfaces in SPR sensing. The main advantage of these nanostructures over smooth metal films for POC diagnostics is that they can be interrogated with white light at normal incidence, greatly simplifying optical instrumentation.[92] Rather than measuring the SPR angle, one instead measures the transmission spectrum through the nanohole array. High numerical aperture optics can be used, so a very large multiplexed array of biosensor probes can be simultaneously imaged. However, the detection limit of the nanohole array technique is poor compared with conventional SPR. In recent microfluidic implementations characterized with glutathione S-transferase (GST)[93] and bovine serum albumin (BSA),[94] the

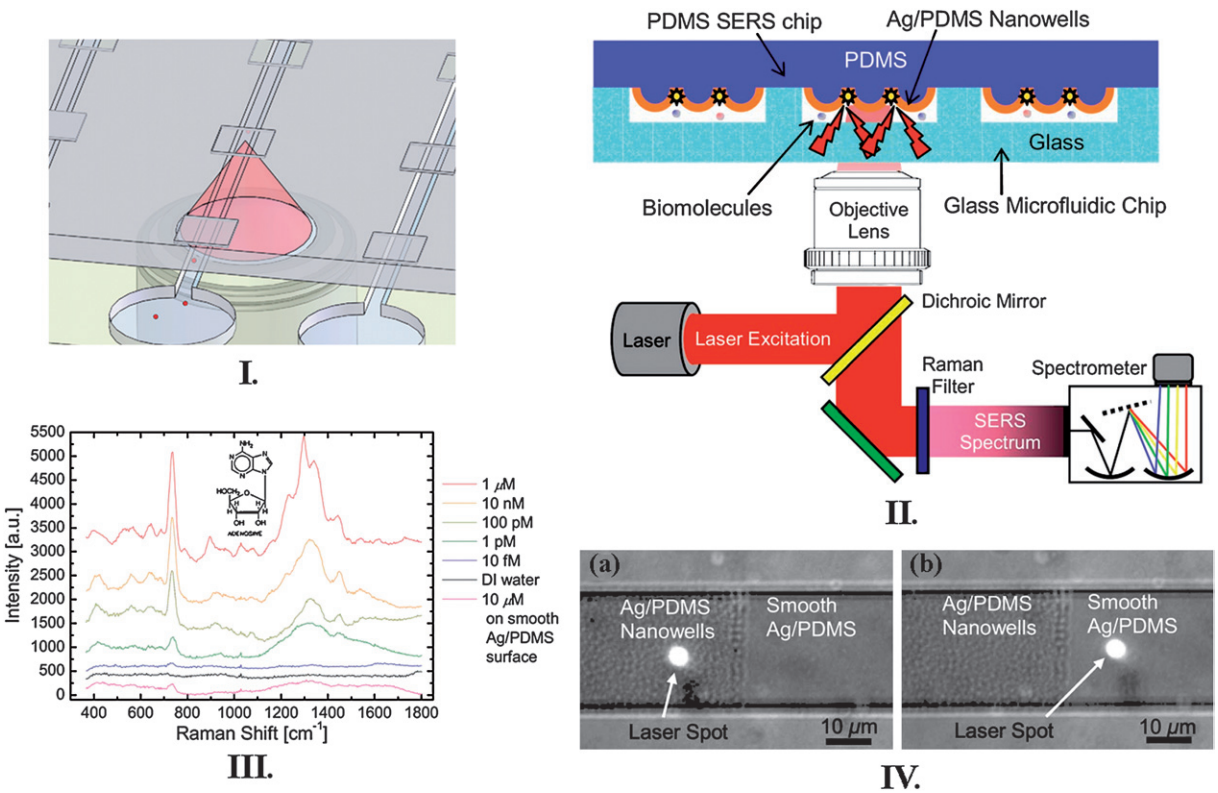

Fig. 20 Integrated nanowell SERS array demonstrating batch fabrication of nanopatterned metallic substrates and microfluidic devices. (I) Conceptual design. (II) Schematic showing optical instrumentation. (III) Resulting Raman spectra from the device with different concentrations of rhodamine 6G. (IV) The device incorporated both patterned and unpatterned Ag substrates to clearly demonstrate the enhancement provided by the patterning method (measured to be 10^7). Reprinted from ref. 98 with permission from the American Institute of Physics.

LODs were 13 nM and 26 nM, respectively. While more work needs to be done to improve the sensitivity of these devices and demonstrate their utility in real biological samples, this is a promising technology for future optical microfluidic POC diagnostic systems.

Surface-enhanced Raman spectroscopy

Raman scattering is an extremely weak phenomenon in which a small fraction of photons impinging on a molecule lose some of their energy to one or more quantum vibrational modes in the molecule and thereby scatter inelastically, leading to a spectrum of lower energy (Stokes-shifted) peaks which can help uniquely identify the molecule. Raman spectroscopy is commonly used in analytical chemistry with large cuvet volumes, powerful lasers, and precision optics, but certain LSPR substrate geometries which include nanoscale gaps or sharp features exhibit extremely high electric field intensities in their adjacent volumes, giving rise to a dramatic increase in the intensity of Raman scattering for molecules located within these volumes. This technique, called surface-enhanced Raman scattering (SERS), was first discovered by Fleischmann *et al.* in 1974[95] with the use of a roughened silver substrate. More recently, nanoengineered LSPR substrates have been applied to achieve even greater Raman enhancement.[96,97] Liu and Lee demonstrated a batch-fabrication process for patterned SERS substrates in microfluidic devices with enhancement factors 10^7 times greater than unpatterned (*i.e.* smooth metal) substrates (Fig. 20).[98] Most research incorporating SERS substrates in microfluidic devices focuses on either characterizing new substrates (typically using model Raman analytes like Rhodamine 6G) or on detecting small organic molecule analytes for environmental, defense, and industrial applications.[99] A few examples of DNA hybridization[100,101] and bacteria detection[102] exist. But as with LSPR-based sensors, portable diagnostic systems have been slow to emerge.

Many SERS biosensors employ reporter molecules with strong, distinct Raman spectra to label molecules of interest. This means that, as with QDs, spectral multiplexing may be achievable while using the same excitation wavelength. When used in a sandwich assay configuration where capture probes are attached to a SERS substrate, these SERS labels will only be visible when they are brought in close proximity to the substrate (*i.e.* by antigen/antibody conjugation or DNA hybridization). This may provide an advantage over fluorophores or other labels for POC systems, because it virtually eliminates background signal from unbound labels, thus boosting sensitivity. Also, as with UPTs, SERS excitation is typically done in the near IR range, where interference from biological media is minimal. These two advantages may obviate the need for a washing step, decreasing procedural complexity. Furthermore, SERS nanoparticle tags have been demonstrated with sensitivities one order of magnitude greater than those of fluorophores.[103]

A variation of SERS, surface-enhanced resonance Raman scattering (SERRS), involves the resonant excitation of a molecule to an excited electronic state, and adds an additional factor of 100–1000 to scattering enhancement. Oxonica (formerly Nanoplex Technologies) has commercialized the first SERRS-based POC immunoassay. The device consists of a disposable LFA containing glass-coated nanoparticles which feature a gold core coated with a SERRS reporter molecule.[104] Thanks to the glass coating, these particles are extremely robust and show a readily identifiable spectral signature no matter what media they are in or what molecules are bound to their surface. Oxonica produces a variety of SERRS tags with unique spectra, enabling simple multiplexing on the same LFA strip. They demonstrate a >10× sensitivity increase over conventional lateral flow immunoassays for the subtyping of influenza. The company is also pursuing bench-top ELISA devices which use SERRS labels rather than fluorophores for a one-step, no-wash assay.

It is also possible to achieve label-free, probe-free detection of certain pathogens using SERS. Shanmukth *et al.* demonstrated that SERS could be used to uniquely identify different respiratory viruses, and even different strains of the same virus, without using antibodies or labels.[105] Measurements were performed in filtered cell lysate, and it was shown that distinct Raman peaks could be observed which corresponded to different viruses and viral strains due to their unique surface proteins (Fig. 21). Although reliable diagnostics will most likely always require

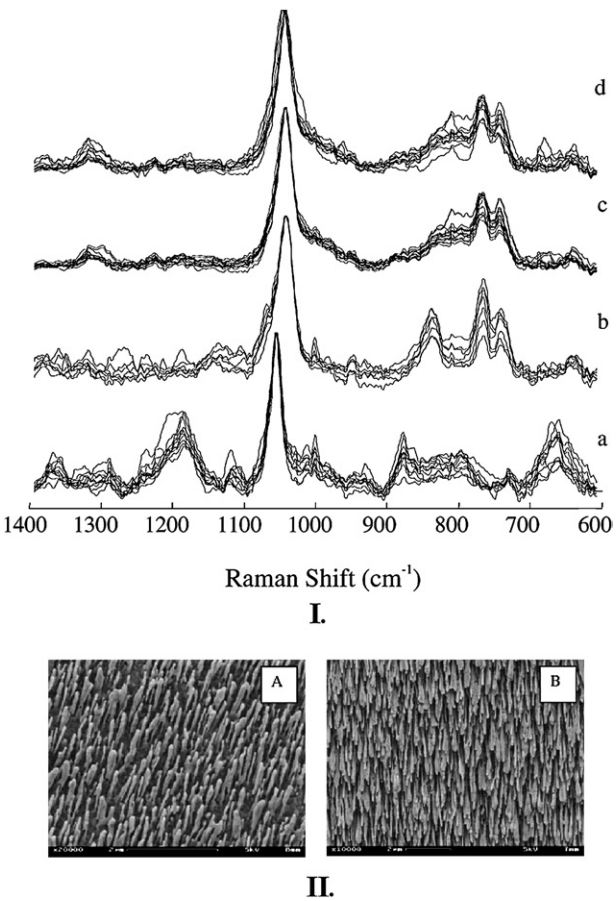

Fig. 21 Label-free, probe-free SERS detection of different respiratory syncytial virus strains. (I) Each viral strain shows a unique SERS "fingerprint" spectrum. (a) Strain A/long, (b) strain B1, (c) strain A2 with G gene deletion, (d) strain A2. (II) SEM images showing Ag nanorod substrates with different lengths, (A) 868 nm and (B) 2080 nm. Reprinted from ref. 105 with permission from the American Chemical Society.

capture probe molecules, these results indicate that SERS can be used as an additional, orthogonal layer of detection which can help discriminate between specifically- and non-specifically-bound ligands.

Many groups have strived to understand the physical basis for SERS in order to develop better substrates, and several reviews are available on this subject.[97,99] Although still a very young technology, SERS shows promise in POC diagnostics because of its ability to provide information-rich spectra which can lead to highly specific molecular identification. As with LSPR sensing, the challenge lies in producing sufficiently uniform nano-structures and low-cost portable spectrometers which provide sufficient spectral resolution.

Conclusions

Optical detection remains the most powerful technique for genomic and proteomic analysis in microfluidics, and integrating sensitive optical systems that are robust and inexpensive remains an ongoing challenge. Many groups have addressed this by building portable versions of conventional instruments (such as fluorimeters and spectrometers), while others have instead attempted to integrate some or all of the detection hardware on the microfluidic device itself. Still others are exploring nano-photonic probes and plasmonics to enable entirely new detection paradigms. A variety of label-free detection techniques have been explored which may reduce the number of reagents and fluid handling steps required to perform an assay and hold great promise for POC diagnostics.

A variety of the techniques illustrated here measure analyte binding at a surface and have the advantage that they are less sensitive to interference from non-specific molecules in the bulk fluid. But, these techniques require surface functionalization which can increase cost, reduce shelf life, and introduce manufacturing variability to the device. Volumetric measurement techniques, on the other hand, are much simpler to implement, but they tend to suffer from shorter optical path lengths and are more susceptible to non-specific interference.

As device integration improves, there is likely to be a push for greater orthogonality in testing, potentially incorporating both proteomic and genomic detection, along with multiple detection mechanisms. In this regard, spectroscopic molecular recognition technologies like SERS are very attractive because they can add another layer of confirmation over conventional chromatography or labeling techniques.

The optical detection techniques reviewed here have significant potential for integration into the next-generation of POC devices which will undoubtedly have a substantial impact on global health, clinical diagnostics, and emergency medicine. Future efforts will likely involve the integration of optical detection systems within automated microfluidic platforms which incorporate sample preparation from raw biological samples (*e.g.* whole blood or saliva). As these technologies move closer to commercial viability, there will be an emphasis on using conventional mass fabrication processes and materials (such as injection molding of thermoplastics). Although PDMS is ideal for quick prototyping and exhibits excellent optical properties (low autofluorescence and high transmissivity), it may not be a good candidate for mass fabrication. Finally, as the optoelectronics industry continues to drive down the cost and improve the quality of components like diode lasers and CCD image sensors, leveraging these off-the-shelf technologies will be key to realizing practical POC diagnostic devices.

Acknowledgements

The authors would like to thank Rick Henrikson, Tanner Nevill, David Breslauer, Ben Ross, and Adrian Sprenger for helpful discussions. FBM gratefully acknowledges the support of an NDSEG fellowship.

References

1 A. Dupuy, S. Lehmann and J. Cristol, *Clinical Chemistry and Laboratory Medicine*, 2005, **43**, 1291–1302.
2 L. Bissonnette and M. Bergeron, *Expert Review of Medical Diagnostics*, 2006, **6**, 433–450.
3 C. D. Chin, V. Linder and S. K. Sia, *Lab Chip*, 2007, **7**, 41–57.
4 P. Yager, T. Edwards, E. Fu, K. Helton, K. Nelson, M. R. Tam and B. H. Weigl, *Nature*, 2006, **442**, 412–418.
5 K. M. Horsman, J. M. Bienvenue, K. R. Blasier and J. P. Landers, *Journal of Forensic Sciences*, 2007, **52**, 784–799.
6 G. M. Whitesides, *Nature*, 2006, **442**, 368–373.
7 F. Rouet, D. K. Ekouevi, M. Chaix, M. Burgard, A. Inwoley, T. D. Tony, C. Danel, X. Anglaret, V. Leroy, P. Msellati, F. Dabis and C. Rouzioux, *J. Clin. Microbiol.*, 2005, **43**, 2709–2717.
8 H. Park, H. Jang, E. Song, C. L. Chang, M. Lee, S. Jeong, J. Park, B. Kang and C. Kim, *J. Clin. Microbiol.*, 2005, **43**, 1782–1788.
9 D. Psaltis, S. R. Quake and C. Yang, *Nature*, 2006, **442**, 381–386.
10 Hunt and Wilkinson, *Microfluidics and Nanofluidics*, 2008, **4**, 53–79.
11 A. Llobera, S. Demming, R. Wilke and S. Buttgenbach, *Lab Chip*, 2007, **7**, 1560–1566.
12 K. Ro, K. Lim, B. Shim and J. Hahn, *Anal. Chem.*, 2005, **77**, 5160–5166.
13 J. Steigert, M. Grumann, T. Brenner, L. Riegger, J. Harter, R. Zengerle and J. Ducree, *Lab Chip*, 2006, **6**, 1040–1044.
14 Y. Li, L. M. L. Ou and H. Yu, *Anal. Chem.*, 2008.
15 J. J. La Clair and M. D. Burkart, *Org. Biomol. Chem.*, 2003, **1**, 3244–9.
16 O. Gustafsson, K. B. Mogensen, P. D. Ohlsson, Y. Liu, S. C. Jacobson and J. P. Kutter, *Journal of Micromechanics and Microengineering*, 2008, **18**, 055021.
17 http://www.nanogen.com/products/ilynxreader/.
18 http://www.cholestech.com/docs/gdx/Technical Focus GDX Specifications.pdf.
19 F. Xu, P. Datta, H. Wang, S. Gurung, M. Hashimoto, S. Wei, J. Goettert, R. McCarley and S. Soper, *Anal. Chem.*, 2007, **79**, 9007–9013.
20 P. Liu, T. Seo, N. Beyor, K. Shin, J. Scherer and R. Mathies, *Anal. Chem.*, 2007, **79**, 1881–1889.
21 D. Liu, X. Zhou, R. Zhong, N. Ye, G. Chang, W. Xiong, X. Mei and B. Lin, *Talanta*, 2006, **68**, 616–622.
22 A. E. Herr, A. V. Hatch, W. V. Giannobile, D. J. Throckmorton, H. M. Tran, J. S. Brennan and A. K. Singh, *Ann. N.Y. Acad.Sci.*, 2007, **1098**, 362–374.
23 J. Seo and L. P. Lee, in *IEEE Transducers 2003: The 12th International Conference on Solid-State Sensors, Actuators and Microsystems*, 2003, vol. 2, pp. 1136–1139.
24 J. Seo and L. P. Lee, *Sensors and Actuators B: Chemical*, 2004, **99**, 615–622.
25 W. Du, Q. Fang, Q. He and Z. Fang, *Anal. Chem.*, 2005, **77**, 1330–1337.
26 T. Zhang, Q. Fang, S. Wang, L. Qin, P. Wang, Z. Wu and Z. Fang, *Talanta*, 2005, **68**, 19–24.
27 K. Miyaki, Y. Guo, T. Shimosaka, T. Nakagama, H. Nakajima and K. Uchiyama, *Analytical and Bioanalytical Chemistry*, 2005, **382**, 810–816.
28 O. Hofmann, X. Wang, A. Cornwell, S. Beecher, A. Raja, D. D. C. Bradley, A. J. deMello and J. C. deMello, *Lab Chip*, 2006, **6**, 981–987.

29 C. L. Bliss, J. N. McMullin and C. J. Backhouse, *Lab Chip*, 2007, **7**, 1280–1287.
30 O. Schmidt, M. Bassler, P. Kiesel, C. Knollenberg and N. Johnson, *Lab Chip*, 2007, **7**, 626–629.
31 D. Vezenov, B. Mayers, R. Conroy, G. Whitesides, P. Snee, Y. Chan, D. Nocera and M. Bawendi, *J. Am. Chem. Soc.*, 2005, **127**, 8952–8953.
32 S. Balslev, A. M. Jorgensen, B. Bilenberg, K. B. Mogensen, D. Snakenborg, O. Geschke, J. P. Kutter and A. Kristensen, *Lab Chip*, 2006, **6**, 213–217.
33 J. A. Chediak, Z. Luo, J. Seo, N. Cheung, L. P. Lee and T. D. Sands, *Sensors and Actuators A: Physical*, 2004, **111**, 1–7.
34 A. Pais, A. Banerjee, D. Klotzkin and I. Papautsky, *Lab Chip*, 2008, **8**, 794–800.
35 A. E. Herr, A. V. Hatch, D. J. Throckmorton, H. M. Tran, J. S. Brennan, W. V. Giannobile and A. K. Singh, *Proceedings of the National Academy of Sciences*, 2007, **104**, 5268–5273.
36 N. Christodoulides, S. Mohanty, C. S. Miller, M. C. Langub, P. N. Floriano, P. Dharshan, M. F. Ali, B. Bernard, D. Romanovicz, E. Anslyn, P. C. Fox and J. T. McDevitt, *Lab Chip*, 2005, **5**, 261–269.
37 A. Woolley, D. Hadley, P. Landre, A. deMello, R. Mathies and M. Northrup, *Anal. Chem.*, 1996, **68**, 4081–4086.
38 F. Huang, C. Liao and G. Lee, *Electrophoresis*, 2006, **27**, 3297–3305.
39 C. J. Easley, J. M. Karlinsey, J. M. Bienvenue, L. A. Legendre, M. G. Roper, S. H. Feldman, M. A. Hughes, E. L. Hewlett, T. J. Merkel, J. P. Ferrance and J. P. Landers, *Proceedings of the National Academy of Sciences*, 2006, **103**, 19272–19277.
40 M. Hashimoto, F. Barany and S. A. Soper, *Biosensors and Bioelectronics*, 2006, **21**, 1915–1923.
41 Z. Wang, A. Sekulovic, J. P. Kutter, D. D. Bang and A. Wolff, *Electrophoresis*, 2006, **27**, 5051–5058.
42 M. C. Smith, G. Steimle, S. Ivanov, M. Holly and D. P. Fries, *Analytica Chimica Acta*, 2007, **598**, 286–294.
43 S. Kedia, S. A. Samson, A. Farmer, M. C. Smith, D. Fries and S. Bhansali, *Proceedings of the SPIE: Smart Structures, Devices, and Systems II*, 2005, **vol. 5649**, 241–252.
44 A. Bhattacharyya and C. Klapperich, *Biomedical Microdevices*, 2007, **9**, 245–251.
45 E. Yacoub-George, W. Hell, L. Meixner, F. Wenninger, K. Bock, P. Lindner, H. Wolf, T. Kloth and K. A. Feller, *Biosensors and Bioelectronics*, 2007, **22**, 1368–1375.
46 G. Marchand, P. Broyer, V. Lanet, C. Delattre, F. Foucault, L. Menou, B. Calvas, D. Roller, F. Ginot, R. Campagnolo and F. Mallard, *Biomedical Microdevices*, 2008, **10**, 35–45.
47 A. Ymeti, J. Greve, P. Lambeck, T. Wink, S. vanHovell, T. Beumer, R. Wijn, R. Heideman, V. Subramaniam and J. Kanger, *Nano Lett.*, 2007, **7**, 394–397.
48 J. Xu, D. Suarez and D. Gottfried, *Analytical and Bioanalytical Chemistry*, 2007, **389**, 1193–1199.
49 F. J. Blanco, M. Agirregabiria, J. Berganzo, K. Mayora, J. Elizalde, A. Calle, C. Dominguez and L. M. Lechuga, *Journal of Micromechanics and Microengineering*, 2006, **16**, 1006–1016.
50 F. Pröll, B. Möhrle, M. Kumpf and G. Gauglitz, *Analytical and Bioanalytical Chemistry*, 2005, **382**, 1889–1894.
51 C. Albrecht, N. Kaeppel and G. Gauglitz, *Analytical and Bioanalytical Chemistry*, 2008, **391**, 1845–1852.
52 D. Markov, K. Swinney and D. Bornhop, *J. Am. Chem. Soc.*, 2004, **126**, 16659–16664.
53 D. J. Bornhop, J. C. Latham, A. Kussrow, D. A. Markov, R. D. Jones and H. S. Sorensen, *Science*, 2007, **317**, 1732–1736.
54 T. M. Chinowsky, J. G. Quinn, D. U. Bartholomew, R. Kaiser and J. L. Elkind, *Sensors and Actuators B: Chemical*, 2003, **91**, 266–274.
55 J. Waswa, J. Irudayaraj and C. DebRoy, *LWT —Food Science and Technology*, 2007, **40**, 187–192.
56 D. Wei, O. A. Oyarzabal, T. Huang, S. Balasubramanian, S. Sista and A. L. Simonian, *Journal of Microbiological Methods*, 2007, **69**, 78–85.
57 T. M. Chinowsky, M. S. Grow, K. S. Johnston, K. Nelson, T. Edwards, E. Fu and P. Yager, *Biosensors and Bioelectronics*, 2007, **22**, 2208–2215.
58 E. Fu, T. Chinowsky, K. Nelson, K. Johnston, T. Edwards, K. Helton, M. Grow, J. Miller and P. Yager, *Oral-Based Diagnostics*, 2007, **1098**, 335–344.
59 T. M. Chinowsky, S. D. Soelberg, P. Baker, N. R. Swanson, P. Kauffman, A. Mactutis, M. S. Grow, R. Atmar, S. S. Yee and C. E. Furlong, *Biosensors and Bioelectronics*, 2007, **22**, 2268–2275.
60 B. Feltis, B. Sexton, F. Glenn, M. Best, M. Wilkins and T. Davis, *Biosensors and Bioelectronics*, 2008, **23**, 1131–1136.
61 Y. Luo, F. Yu and R. N. Zare, *Lab Chip*, 2008, **8**, 694–700.
62 J. Klostranec and W. Chan, *Advanced Materials*, 2006, **18**, 1953–1964.
63 J. Klostranec, Q. Xiang, G. Farcas, J. Lee, A. Rhee, E. Lafferty, S. Perrault, K. Kain and W. Chan, *Nano Lett.*, 2007, **7**, 2812–2818.
64 P. Eastman, W. Ruan, M. Doctolero, R. Nuttall, G. deFeo, J. Park, J. Chu, P. Cooke, J. Gray, S. Li and F. Chen, *Nano Lett.*, 2006, **6**, 1059–1064.
65 K. Yun, D. Lee, H. Kim and E. Yoon, *Measurement Science and Technology*, 2006, **17**, 3178–3183.
66 W. Liu, L. Zhu, Q. Qin, Q. Zhang, H. Feng and S. Ang, *Lab Chip*, 2005, **5**, 1327–1330.
67 L. J. Lucas, J. N. Chesler and J. Yoon, *Biosensors and Bioelectronics*, 2007, **23**, 675–681.
68 Z. Yan, L. Zhou, Y. Zhao, J. Wang, L. Huang, K. Hu, H. Liu, H. Wang, Z. Guo, Y. Song, H. Huang and R. Yang, *Sensors and Actuators B: Chemical*, 2006, **119**, 656–663.
69 J. Wang, Z. Chen, P. L. A. M. Corstjens, M. G. Mauk and H. H. Bau, *Lab Chip*, 2006, **6**, 46–53.
70 P. L. A. M. Corstjens, Z. Chen, M. Zuiderwijk, H. H. Bau, W. R. Abrams, D. Malamud, R. S. Niedbala and H. J. Tanke, *Annals of the New York Academy of Sciences*, 2007, **1098**, 437–445.
71 W. Abrams, C. Barber, K. McCann, G. Tong, Z. Chen, M. Mauk, J. Wang, A. Volkov, P. Bourdelle, P. Corstjensd, M. Zuiderwijk, K. Kardos, S. Li, H. Tanke, R. Niedbala, D. Malamud and H. Bau, *Oral-Based Diagnostics*, 2007, **1098**, 375–388.
72 T. A. Taton, C. A. Mirkin and R. L. Letsinger, *Science*, 2000, **289**, 1757–1760.
73 J. Nam, C. S. Thaxton and C. A. Mirkin, *Science*, 2003, **301**, 1884–1886.
74 P. Jain, X. Huang, I. El-Sayed and M. El-Sayed, *Plasmonics*, 2007, **2**, 107–118.
75 J. N. Anker, W. P. Hall, O. Lyandres, N. C. Shah, J. Zhao and R. P. Van Duyne, *Nat Mater*, 2008, **7**, 442–453.
76 M. Stewart, C. Anderton, L. Thompson, J. Maria, S. Gray, J. Rogers and R. Nuzzo, *Chem. Rev.*, 2008, **108**, 494–521.
77 C. Yonzon, E. Jeoung, S. Zou, G. Schatz, M. Mrksich and R. VanDuyne, *J. Am. Chem. Soc.*, 2004, **126**, 12669–12676.
78 K. M. Mayer, S. Lee, H. Liao, B. C. Rostro, A. Fuentes, P. T. Scully, C. L. Nehl and J. H. Hafner, *ACS Nano*, 2008, **2**, 687–692.
79 C. Haynes and R. Van Duyne, *J. Phys. Chem. B*, 2001, **105**, 5599–5611.
80 G. Liu, Y. Lu, J. Kim, J. Doll and L. Lee, *Advanced Materials*, 2005, **17**, 2683–2688.
81 Y. B. Zheng, B. K. Juluri, X. Mao, T. R. Walker and T. J. Huang, *J. Appl. Phys.*, 2008, **103**, 014308–9.
82 T. Endo, K. Kerman, N. Nagatani, H. Hiepa, D. Kim, Y. Yonezawa, K. Nakano and E. Tamiya, *Anal. Chem.*, 2006, **78**, 6465–6475.
83 H. Minh Hiep, T. Endo, K. Kerman, M. Chikae, D. Kim, S. Yamamura, Y. Takamura and E. Tamiya, *Science and Technology of Advanced Materials*, 2007, **8**, 331–338.
84 L. Sherry, R. Jin, C. Mirkin, G. Schatz and R. VanDuyne, *Nano Lett.*, 2006, **6**, 2060–2065.
85 T. Lin, K. Huang and C. Liu, *Biosensors and Bioelectronics*, 2006, **22**, 513–518.
86 C. Schofield, R. Field and D. Russell, *Anal. Chem.*, 2007, **79**, 1356–1361.
87 S. Marinakos, S. Chen and A. Chilkoti, *Anal. Chem.*, 2007, **79**, 5278–5283.
88 S. Bishnoi, C. Rozell, C. Levin, M. Gheith, B. Johnson, D. Johnson and N. Halas, *Nano Lett.*, 2006, **6**, 1687–1692.
89 H. Wang, D. Brandl, F. Le, P. Nordlander and N. Halas, *Nano Lett.*, 2006, **6**, 827–832.
90 D. Kim, K. Kerman, M. Saito, R. Sathuluri, T. Endo, S. Yamamura, Y. Kwon and E. Tamiya, *Anal. Chem.*, 2007, **79**, 1855–1864.
91 H. M. Hiep, T. Nakayama, M. Saito, S. Yamamura, Y. Takamura and E. Tamiya, *Jpn. J. Appl. Phys.*, 2008, **47**, 1337–1341.
92 A. DeLeebeeck, L. Kumar, V. deLange, D. Sinton, R. Gordon and A. Brolo, *Anal. Chem.*, 2007, **79**, 4094–4100.

93 J. Ji, J. O'Connell, D. Carter and D. Larson, *Anal. Chem.*, 2008, **80**, 2491–2498.
94 L. Pang, G. M. Hwang, B. Slutsky and Y. Fainman, *Appl. Phys. Lett.*, 2007, **91**, 123112–3.
95 M. Fleischmann, P. J. Hendra and A. J. McQuillan, *Chemical Physics Letters*, 1974, **26**, 163–166.
96 K. A. Willets and R. P. Van Duyne, *An. Rev. Phys. Chem.*, 2007, **58**, 267–297.
97 M. J. Banholzer, J. E. Millstone, L. Qin and C. A. Mirkin, *Chem. Soc. Rev.*, 2008, **37**, 885–897.
98 G. L. Liu and L. P. Lee, *Appl. Phys. Lett.*, 2005, **87**, 074101–3.
99 L. Chen and J. Choo, *Electrophoresis*, 2008, **29**, 1815–1828.
100 P. Monaghan, K. McCarney, A. Ricketts, R. Littleford, F. Docherty, W. Smith, D. Graham and J. Cooper, *Anal. Chem.*, 2007, **79**, 2844–2849.
101 M. Sha, S. Penn, G. Freeman and W. Doering, *NanoBioTechnology*, 2007, **3**, 23–30.
102 D. Hou, S. Maheshwari and Hsueh-Chia Chang, *Biomicrofluidics*, 2007, **1**, N.PAG.
103 G. Sabatte, R. Keir, M. Lawlor, M. Black, D. Graham and W. Smith, *Anal. Chem.*, 2008, **80**, 2351–2356.
104 S. Mulvaney, M. Musick, C. Keating and M. Natan, *Langmuir*, 2003, **19**, 4784–4790.
105 S. Shanmukh, L. Jones, J. Driskell, Y. Zhao, R. Dluhy and R. Tripp, *Nano Lett.*, 2006, **6**, 2630–2636.